PROPELLER BLADE ICE ANALYSIS

Vasile PRISACARIU, Adrian PITICAR
"Henri Coandă" Air Force Academy, Brasov, Romania (prisacariu.vasile@afahc.ro, piticar.adrian@afahc.ro)

DOI: 10.19062/1842-9238.2021.19.2.2

Abstract: *Atmospheric phenomena can influence flight safety through a series of manifestations of the air masses in the flight area. Such a dangerous manifestation is the icing that can seriously affect the performance of aircraft and lead to flight events. The article draws attention to the phenomenon of icing as located on propellers, a phenomenon which is analyzed on both a 2D (aerodynamic profile) and a three-dimensional (three-blade propeller) geometry, using the Qblade freeware tool, and in the case of icing formed on the NACA 0009 leading edge. The aerodynamic analysis proposed for comparison provides graphical and numerical data relevant for an assessment of the degree of influence of icing deposits in the analyzed case, the proposed geometries and the generated numerical data can be exported and exploited later, by using software analysis tools.*

Keywords: *icing, NACA 009, Qblade analysis, aircraft propeller.*

Acronyms and symbols

c_l	*Lift coefficient*	*AoA*	*Angle of attack*
c_l/c_d	*Gliding ratio*	β	*Local twist angle*
c_p	*Pressure coefficient / power coefficient*	*T*	*Thrust*
c_d	*Drag coefficient*	ρ	*Air density*
c_m	*Pitch coefficient*	*D*	*Propeller diameter*
b	*chord*	*Q*	*Torsion*
α	*Local angle of attack*	*P*	*Available power*
n	*Rotation (rot/sec)*	c_n	*Normal force coefficient*

1. INTRODUCTION

Icing manifests itself as deposits of transparent or opaque ice that adhere to certain construction components of an aircraft, especially those exposed to stream. Icing can affect the wing, tail, propellers (on the leading edges), antennas, windshield, Pitot tubes, carburetors or intake engines of jet engines, see Fig. 1.1. It can be found in the case of flights in: altocumulus clouds (weak icing) depending on the isotherms in which it flies; altostratus clouds (0^o isotherm); nimbostratus clouds (glass icing); stratocumulus (moderate icing). [1]

The most common forms of icing that are dangerous for flight safety are: in the form of frost, sometimes with moderate intensity (amount of super cooled water with values of $0.6 / m^3 < 0 < 1.2$ g/m^3); in the form of ice that rarely appears (glassy ice); the icing in the cumulonimbus clouds and the frontal atmospheric zones have strong intensity (they affect the entire surface of the aircraft). [1]

FIG. 1.1 Ice buildup on aircraft surfaces, [2, 3]

Icing can affect the aerodynamic performances of aircraft depending on the quantity and especially the shape of the ice deposits, the contamination of the aerodynamic surfaces producing changes regarding the aerodynamic coefficients, according to the graphs in Fig. 1.2. According to specialist references [5] the area prone to ice contamination is up to 60% of the blade length, see figure 1.3.

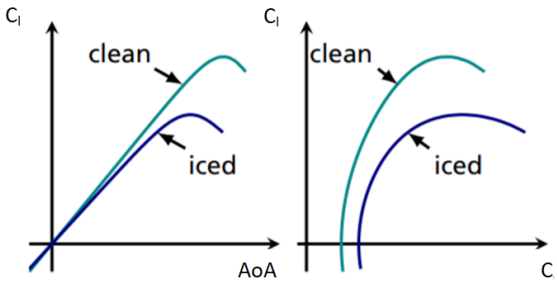

FIG. 1.2 Modification of aerodynamic coefficients due to icing

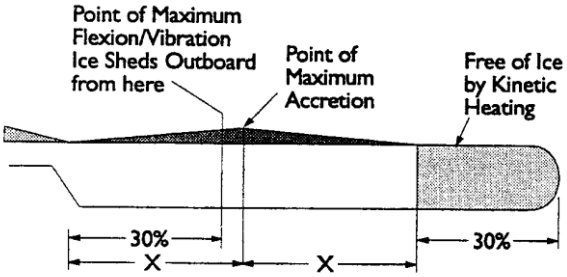

FIG. 1.3 Areas contaminated by ice below freezing point [5]

The favorable temperatures for the icing are for: stable clouds for the range 0^{o}-10^{o}C, in which case the icing appears less frequently for a temperature below -18^{o}C; and for unstable clouds for the range 0^{o}-15^{o}C, but with frequent icing down to -30^{o}C, [5].

The protection of aircrafts against the adverse effects of icing is essential with respect to flight safety. Icing is commonly caused due to the impact of super cooled water with any part of the external structure of an aircraft during flight. Specific warnings for piston propulsion systems icing are not normally included in aviation-specific weather forecasts and pilots need to be prepared to deal with this situation based on their own knowledge and experience. The main objective of this study is to highlight the influence of icing on the propellers of combustion engine-powered aircrafts.

Partial approaches from this study were presented at the ATMOSPHERE AND HYDROSPHERE 2020 conference (fourth edition) at Vatra Dornei organized by Stefan cel Mare University of Suceava. [14].

2. METHODS AND INSTRUMENTS USED IN THE ANALYSIS OF ICING

To highlight the effect of icing on rotating lifting surfaces, a comparative analysis of two clean / frosted theoretical geometries is used in two relevant analysis cases: the two-dimensional case (compared aerodynamic profiles) and the 3D case (compared triple propellers).

The evaluation of the aerodynamic parameters of the frosted / non-frosted airfoils can be done with a series of freeware / trial tools, as follows: Javafoil [6, 7] for 2D geometries, XFLR5 [8, 9] for 2D / 3D geometries, Profiles [10] for 2D geometries, Qblade [4] for 2D / 3D geometries, Flow5 [11] for 2D / 3D geometries, see figure 2.1.

The instrumentation of the aerodynamic analysis in this study is realized by means of the freeware Qblade [4] which offers a geometric module and an aerodynamic analysis module. With the help of the geometric module, airfoils and rotating lifting surfaces (propellers with vertical axis and horizontal axis) can be configured, and the aerodynamic module offers possibilities for multi-parametric numerical analysis.

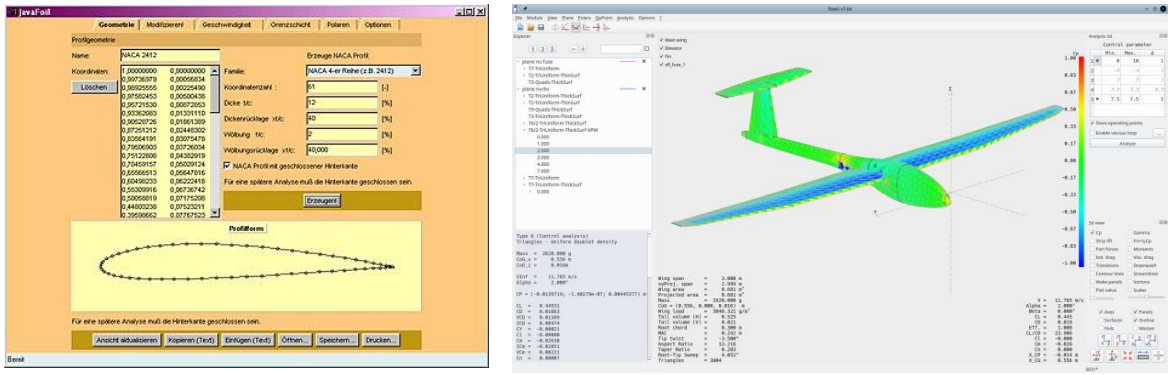

a b

FIG. 2.1 Freeware/trial software, a. Javafoil, b. Flow5.

The proposed comparative aerodynamic analysis provides relevant graphical and numerical data for an assessment of the degree of influence of icing deposits in the analyzed case, the proposed geometries and the generated numerical data can be exported (see annex) and used later using software analysis tools.

3. THEORETICAL ELEMENTS OF ROTARY LIFTING SURFACES

The 3D geometric element subjected to the icing influence analysis is a rotating lifting surface (three blades), having the characteristics shown in Fig. 3.1.

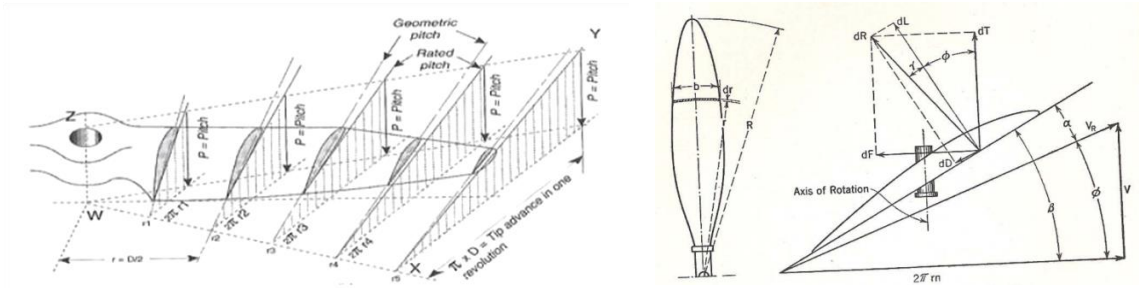

FIG. 3.1 Propeller geometry, [12]

The relevant geometric parameters for our analysis and the characteristic aerodynamic coefficients [12, 13] are as follows:
-power coefficient (c_p) equation 3.1:

$$c_p = \frac{P}{\rho \cdot n^3 \cdot D^5} = 2 \cdot \pi \cdot c_m \qquad 3.1$$

-traction coefficient (c_t) equation 3.2:

$$c_t = \frac{T}{\rho \cdot n^2 \cdot D^5} \qquad 3.2$$

-moment coefficient (c_m) equation 3.3:

$$c_m = \frac{Q}{\rho \cdot n^2 \cdot D^5} \qquad 3.3$$

4. PROPELLER ICING ANALYSIS

4.1 2D analyses

To highlight the influence of icing on a propeller, we chose to perform an aerodynamic analysis on a blade section (aerodynamic profile) NACA 009, in the case of a light (theoretical) icing, which includes the following steps:

a. geometry of the two airfoils, see Fig. 4.1.

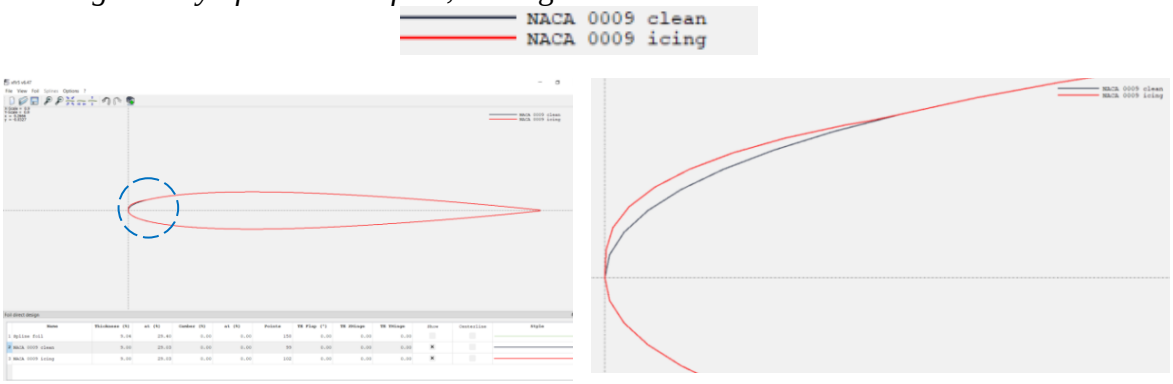

FIG. 4.1. Airfoils for analysis

b.analysis conditions (atmospheric and kinetics), table 4.1:

Table 4.1. Analysis conditions

Parameter	Value	Parameter	Value
Air density	1,225 kg/m^3	Reynolds number	100000
Air viscosity	1,5x10^{-5}	Angle of incidence	-10°... 10°
Analysis	viscous	Boundary layer	yes
Iterations	100		

c. grapho-numerical results and interpretation, see figures 4.2-4.7.

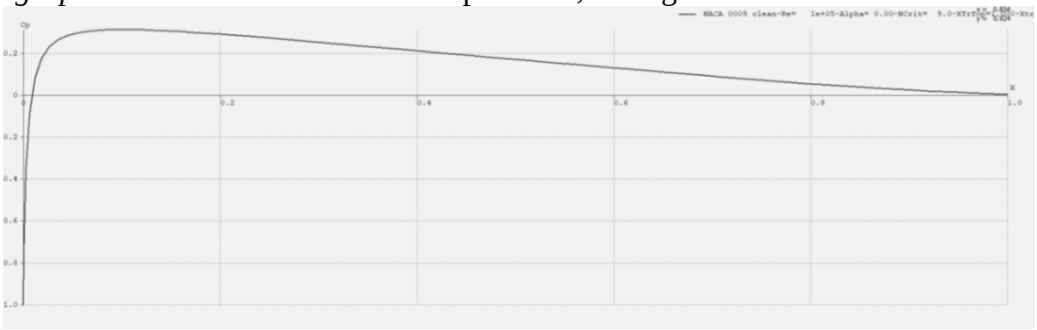

FIG. 4.2 Pressure coefficient distribution (C_p) vs airfoil chord without icing

In the case of the profile not affected by icing (fig.4.2), according to the zero AoA distribution of the pressure coefficient (C_p), the overlapping values for intrados versus extrados are observed due to the symmetrical geometry of the airfoil.

According to the distribution at AoA = 0° of the pressure coefficient C_p at zero angle of attack, it is obvious the creation of an area with turbulent potential on the attack board, due to the irregular geometry in the case of the icing profile (Fig. 4.3).

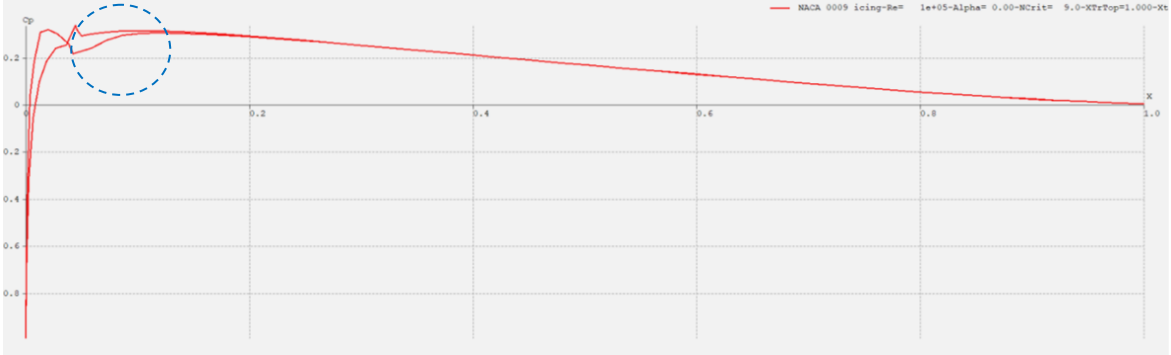

FIG. 4.3 C_p vs airfoil chord with icing for AoA=0°

Figure 4.4 shows an obvious decrease in the values of the lift coefficient (Cl) after the AoA=6° for the airfoil affected by icing, with a $C_{lmaxclean}$ = 0.79 versus $C_{lmaxicing}$ = 0.65 for the AoA=8°. According to figure 4.5 C_d variation, the icing increases the drag especially after the angle of attack of 3°.

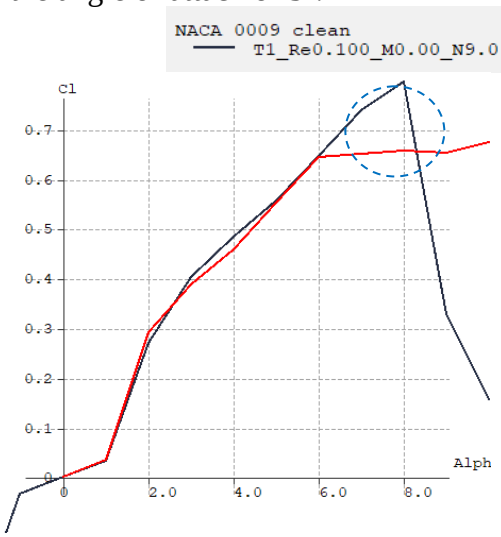

FIG. 4.4 Lfting coefficient variation (C_l) vs AoA (alpha)

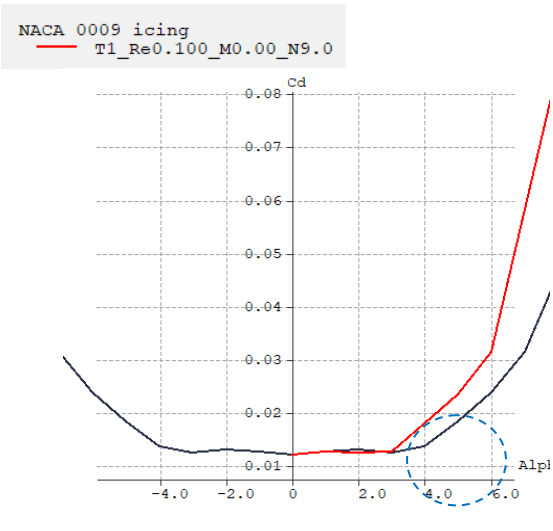

FIG. 4.5 Drag coefficient variation(C_d) vs AoA (alpha)

According to figure 4.6, the icing phenomenon affects the aerodynamic fineness / gliding ratio (C_l/C_d) with the increase of the angle of attack after the value of 3°, which has a direct influence on the decrease of the airfoil efficiency (see figure 4.7).

d. bi-dimensional aerodynamic analysis conclusions

Given the choice of small icing deposits on the leading edge of the airfoil, the comparative analysis of the two geometries shows an alteration of the relevant aerodynamic coefficients, especially after the angle of attack of 3°, AoA at which the airfoil of the propeller blades operates in current mode.

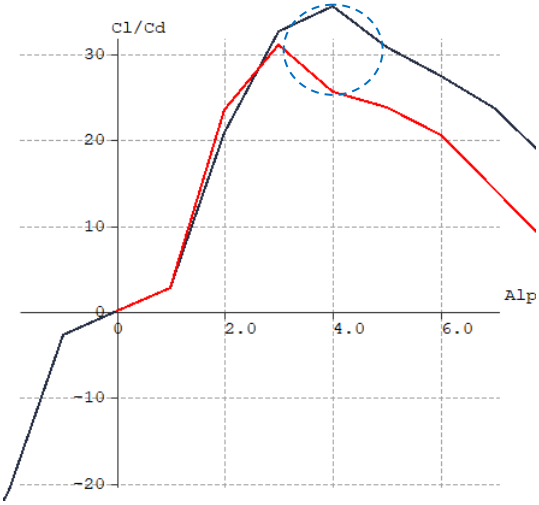

FIG.4.6 Gliding ratio variation (Cl/Cd)) vs AoA (alpha)

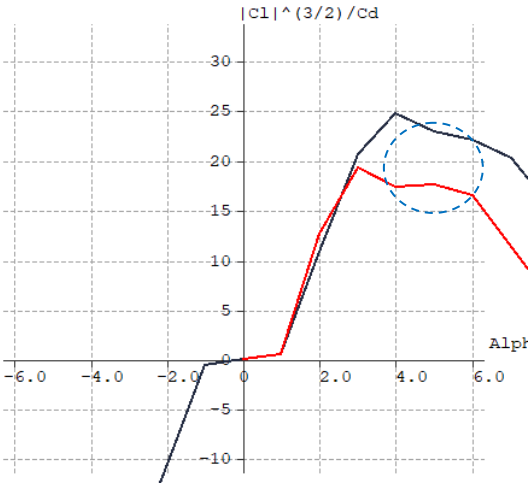

FIG.4.7 Airfoil efficiency variation (Cl^3/Cd^2)) vs AoA (alpha)

4.2. 3D analysis

To highlight the influence of icing on performance on a three-bladed propeller, we chose to perform a three-dimensional aerodynamic analysis on a theoretical geometry, with a slight icing present on the central area of the blade (according to Figure 1.3), the analysis steps being as follows:

a. definition of the theoretical geometry of the two (triple) propellers, having the characteristics and performances from table 4.2, see also figure 4.8.

Table 4.2. Propeller performances and characteristics

Features	Value	Features	Value
Diameter	2100 mm	Hub diameter	100 mm
Blade nmber	3	Airfoil	NACA 009
Blade form	Eliptical	Absolut twist angle	22º

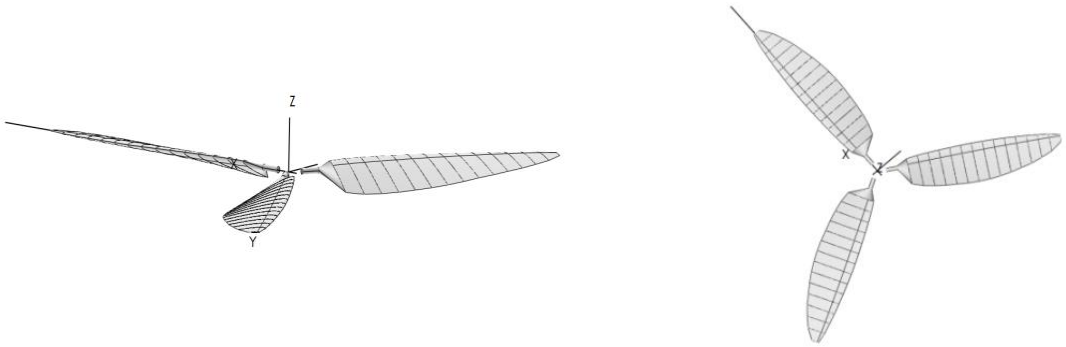

FIG. 4.8 Theoretical propeller for comparative analysis

b. analysis conditions (atmospheric and kinetics), table 4.3:

Table 4.3. Analysis conditions

Parameter	**Value**	**Parameter**	**Value**
Air density	1,225 kg/m^3	Angle of incidence	-10º... 10º
Air viscosity	1,5x10^{-5}	Boundary layer	yes
Analysis	viscous	Iterations	100

c. grapho-numerical results and discussions, see figures 4.9 – 4.10

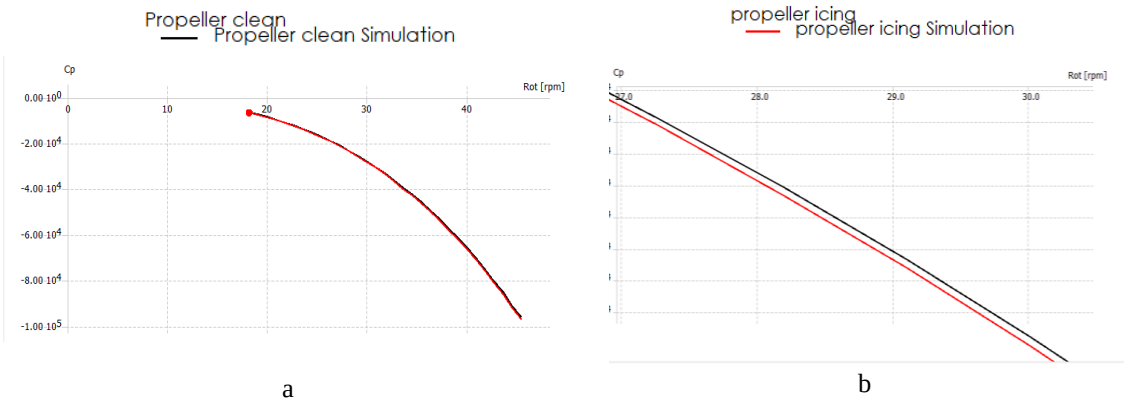

a b

FIG.4.9 Power coefficient variation (C_p) vs rotation speed
(a. whole values interval, b. details)

According to figure 4.9a we observe a similar variation for the two geometries and the decrease of the values of the power coefficient (c_p) over the whole range of the speed value of the propeller (fig. 49b). Figure 4.10 shows a decrease of the traction coefficient (c_t) for the icing propeller geometry over the entire speed range.

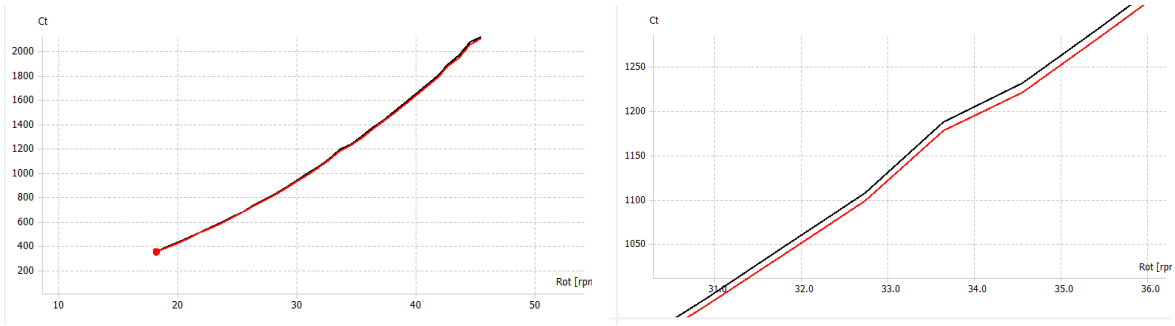

FIG.4.10 Traction coefficient variation (C_t) vs rotation speed
(a. whole values interval, b. details)

The torque coefficient (C_m) has a divergent variation of the values of the two geometries (non-icing / icing propeller) as the rotational speed increases, see figure 4.11.

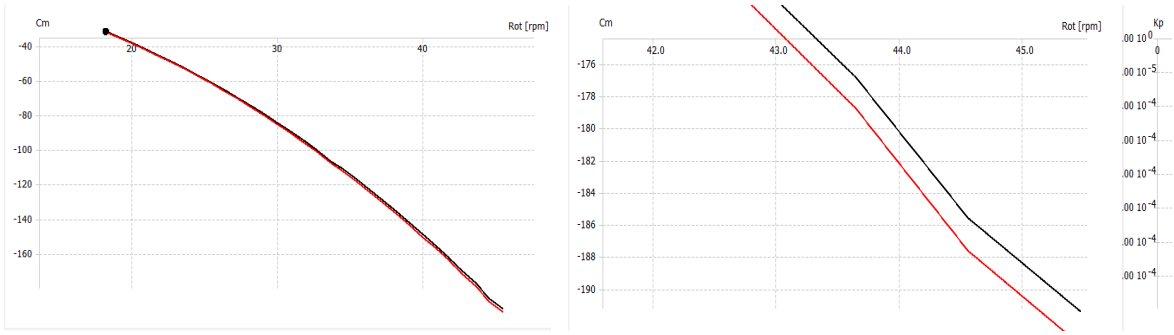

FIG.4.11 Moment coefficient (C_m) vs rotation speed
(a. whole values interval, b. details)

Figure 4.12a shows a decrease in the value of the normal force expressed by the coefficient c_n depending on the local value of the radius (pos/m), the presence of icing in the central area of the blade (0.48 ÷ 0.52 pos/m) indicates a reduction in value characteristic coefficient cn, (see figure 4.12c).

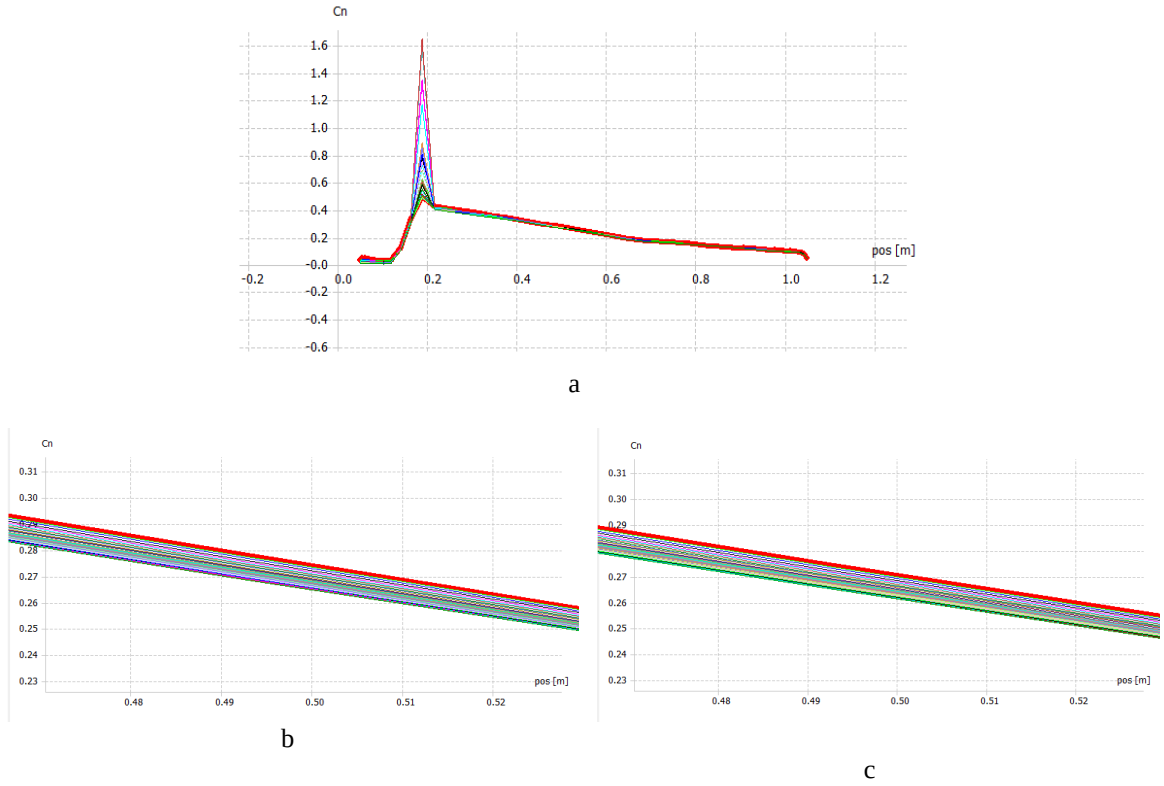

FIG.4.12 Normal axial force coefficient variation (C_n) vs local radius
(a. whole values interval, b. details for non-icing propeller, c. details for icing propeller)

d. conclusions of the 3D aerodynamic analysis

In the case of 3D analysis, a small icing deposition indicates a change in the values of the relevant coefficients, values obtained in the case of theoretical geometries similar to the propellers used by general aviation aircraft.

CONCLUSIONS

The article highlighted the influence of the presence of a small icing deposit defined on the central area of a theoretical propeller using a freeware tool that provides results with a limited degree of confidence in the calculation method and the numerical code used.

The limits of the aerodynamic analysis are influenced both by the degree of reproduction of the icing geometry on the leading edge of the profile and by the degree of confidence of the numerical method that substantiates the approach of the software instrumentation.

The main results revealed a significant influence of icing on the aerodynamic and performance variables of propellers of combustion engine-powered aircrafts. Thus, the lift coefficient, the drag coefficient and the pitch moment coefficient variables were significantly altered in icing contamination leading the aircraft to unstable flight conditions. If no intervention is considered, the risk of flight events is considerably high.

For a refined multi-criteria comparative analysis of icing cases, the instrumentation of a real situation is considered both from an atmospheric and kinetic point of view (aspect transposed in the quantity, area and shape of the icing) and from a geometrically relevant point of view, similar to an aircraft or of a 1: 1 scale construction element.

Future study directions are based on a 2D and 3D geometric parameterization of icing deposits in conditions of atmospheric and kinetic similarity that reproduce scenarios with high degrees of confidence. The 2D and 3D aerodynamic analyzes will use CFD instruments based on finite element methods and will be applied to the actual geometries of the rotating bearing surfaces (propellers) of the operational aircraft.

REFERENCES

[1] Aeroclubul României, *Manual de pregătire teoretică pentru licența de pilot privat PPL(A), Meteorologie*, available at http://aerodromclinceni.ro/wp-content/uploads/2012/07/Meteorologie-2011-v.1.0.pdf;

[2] https://aircrafticing.grc.nasa.gov/1_1_3_4.html , accessed on 12.10.2021;

[3] *Multiphysics icing analysis using HPC Cloud*, https://www.ff4eurohpc.eu/en/success-stories/912/multiphysics_icing_analysis_using_hpc_cloud , accessed on 16.10.2021;

[4] D. Marten, J. Wendler, Qblade guidelines, 2013, available at https://q-blade.org/project_images /files/guidelines_v06.pdf , 76p;

[5] Civil Aviation Authority, *Aircraft Icing Handbook*, version 1, 2000, p108;

[6] M. Hepperle, Javafoil, disponibil la https://www.mh-aerotools.de/airfoils/javafoil.htm, accessed on 12.10.2021;

[7] Prisacariu V., *Aerodynamic analysis of the Clark YH airfoil*, REVIEW OF THE AIR FORCE ACADEMY, 1/2021, Braşov, Romania, ISSN 1842-9238; e-ISSN 2069-4733;

[8] Drela M., Yungren H., *Guidelines for XFLR5 v6.03 (Analysis of foils and wings operating at low Reynolds numbers)*, 2011, available at http://sourceforge.net/projects/xflr5/files;

[9] Prisacariu V., *Aerodynamic analysis of UAVs. MFD Nimbus*, nr. 2(11)/2019, INCAS Bulletin, (P) ISSN 2066-8201, (E) ISSN 2247-4528, DOI: 10.13111/2066-8201.2019.11.2.11, p.135-145;

[10] Duranti S. *Profili 2.21 software*, 2012, Feltre-Italia, www.profili2.com, accessed on 19.10.2021;

[11] Flow5 v7, disponibil la https://flow5.tech/docs/flow5_doc/flow5_doc.html , accessed on 22.10.2021;

[12]W.B. Garner, Model airplane propellers, 2009, 24 p., available at https://www3.nd.edu/~ame40462/garner_Model_Propellers_Article_2009.pdf, accessed on 04.11.2021;

[12] W.B. Garner, Model airplane propellers, 2009, 24 p., available at https://www3.nd.edu/~ame40462/garner_Model_Propellers_Article_2009.pdf, accessed on 04.11.2021;

[13]Propellers, disponibil la https://society-of-flight-test-engineers.github.io/handbook-2013/ propellers.html#propeller-geometry , accesat la data de 04.11.2021;

[14] http://atlas.usv.ro/www/simpozioane/2020/Programul%20Conferintei%20ATMOSFERA%20SI%20HIDROSFERA%20%202020.pdf.

ANEXES

Propeller geometrical data without icing

Blade Export File Created with QBlade v0.96 64bit v0.96 on 20.08.2021 at 20:07:32

Radial Position [m]	Chord Length [m]	Twist [deg]	Pitch Axis Offset [m]	Thread Axis in [% chord]	Airfoil Name
5.00000e-02	2.00000e-02	0.00000e+00	0.00000e+00	2.50000e-01	Circular Foil
1.12500e-01	2.00000e-02	0.00000e+00	0.00000e+00	2.50000e-01	Circular Foil
1.75000e-01	1.70000e-01	-2.60000e+01	0.00000e+00	2.50000e-01	NACA 0009 clean
2.38000e-01	2.00000e-01	-2.40000e+01	0.00000e+00	2.50000e-01	NACA 0009 clean
3.00000e-01	2.15000e-01	-2.20000e+01	0.00000e+00	2.50000e-01	NACA 0009 clean
3.63000e-01	2.25000e-01	-2.00000e+01	0.00000e+00	2.50000e-01	NACA 0009 clean
4.25000e-01	2.30000e-01	-1.80000e+01	0.00000e+00	2.50000e-01	NACA 0009 clean
4.87500e-01	2.35000e-01	-1.60000e+01	0.00000e+00	2.50000e-01	NACA 0009 clean
5.50000e-01	2.35000e-01	-1.40000e+01	0.00000e+00	2.50000e-01	NACA 0009 clean
6.13000e-01	2.30000e-01	-1.20000e+01	0.00000e+00	2.50000e-01	NACA 0009 clean
6.75000e-01	2.20000e-01	-1.00000e+01	0.00000e+00	2.50000e-01	NACA 0009 clean
7.38000e-01	2.05000e-01	-9.00000e+00	0.00000e+00	2.50000e-01	NACA 0009 clean
8.00000e-01	1.85000e-01	-8.00000e+00	0.00000e+00	2.50000e-01	NACA 0009 clean
8.63000e-01	1.65000e-01	-7.00000e+00	0.00000e+00	2.50000e-01	NACA 0009 clean
9.25000e-01	1.35000e-01	-6.00000e+00	0.00000e+00	2.50000e-01	NACA 0009 clean
9.87500e-01	1.00000e-01	-5.00000e+00	0.00000e+00	2.50000e-01	NACA 0009 clean
1.05000e+00	4.00000e-02	-4.00000e+00	0.00000e+00	2.50000e-01	NACA 0009 clean

Propeller geometrical data with icing

QBlade Export File Created with QBlade v0.96 64bit v0.96 on 26.01.2022 at 21:14:59

Radial Position [m]	Chord Length [m]	Twist [deg]	Pitch Axis Offset [m]	Thread Axis in [% chord]	Airfoil Name
5.00000e-02	2.00000e-02	0.00000e+00	0.00000e+00	2.50000e-01	Circular Foil
1.12500e-01	2.00000e-02	0.00000e+00	0.00000e+00	2.50000e-01	Circular Foil
1.75000e-01	1.70000e-01	-2.60000e+01	0.00000e+00	2.50000e-01	NACA 0009 clean
2.38000e-01	2.00000e-01	-2.40000e+01	0.00000e+00	2.50000e-01	NACA 0009 clean
3.00000e-01	2.15000e-01	-2.20000e+01	0.00000e+00	2.50000e-01	NACA 0009 clean
3.63000e-01	2.25000e-01	-2.00000e+01	0.00000e+00	2.50000e-01	NACA 0009 clean
4.25000e-01	2.30000e-01	-1.80000e+01	0.00000e+00	2.50000e-01	NACA 0009 icing
4.87500e-01	2.35000e-01	-1.60000e+01	0.00000e+00	2.50000e-01	NACA 0009 icing
5.50000e-01	2.35000e-01	-1.40000e+01	0.00000e+00	2.50000e-01	NACA 0009 icing
6.13000e-01	2.30000e-01	-1.20000e+01	0.00000e+00	2.50000e-01	NACA 0009 icing
6.75000e-01	2.20000e-01	-1.00000e+01	0.00000e+00	2.50000e-01	NACA 0009 icing
7.38000e-01	2.05000e-01	-9.00000e+00	0.00000e+00	2.50000e-01	NACA 0009 icing
8.00000e-01	1.85000e-01	-8.00000e+00	0.00000e+00	2.50000e-01	NACA 0009 icing
8.63000e-01	1.65000e-01	-7.00000e+00	0.00000e+00	2.50000e-01	NACA 0009 clean
9.25000e-01	1.35000e-01	-6.00000e+00	0.00000e+00	2.50000e-01	NACA 0009 clean
9.87500e-01	1.00000e-01	-5.00000e+00	0.00000e+00	2.50000e-01	NACA 0009 clean
1.05000e+00	4.00000e-02	-4.00000e+00	0.00000e+00	2.50000e-01	NACA 0009 clean

C_p vs rotation

Export File Created with QBlade v0.96 64bit on 26.01.2022 at 20:59:59

Propeller clean Simulation		propeller icing Simulation	
Rot [rpm]	Cp	Rot [rpm]	Cp
1.81891e+01	-6.27941e+03	1.81891e+01	-6.34570e+03
1.90986e+01	-7.25669e+03	1.90986e+01	-7.33349e+03
2.00080e+01	-8.32650e+03	2.00080e+01	-8.41478e+03
2.09175e+01	-9.49930e+03	2.09175e+01	-9.60017e+03
2.18270e+01	-1.08242e+04	2.18270e+01	-1.09388e+04
2.27364e+01	-1.21646e+04	2.27364e+01	-1.22941e+04
2.36459e+01	-1.36667e+04	2.36459e+01	-1.38124e+04
2.45553e+01	-1.52863e+04	2.45553e+01	-1.54495e+04
2.54648e+01	-1.70279e+04	2.54648e+01	-1.72101e+04
2.63742e+01	-1.89005e+04	2.63742e+01	-1.91030e+04
2.72837e+01	-2.09003e+04	2.72837e+01	-2.11247e+04
2.81932e+01	-2.30382e+04	2.81932e+01	-2.32859e+04
2.91026e+01	-2.53227e+04	2.91026e+01	-2.55953e+04
3.00121e+01	-2.77445e+04	3.00121e+01	-2.80437e+04
3.09215e+01	-3.03256e+04	3.09215e+01	-3.06530e+04
3.18310e+01	-3.30624e+04	3.18310e+01	-3.34196e+04
3.27404e+01	-3.59532e+04	3.27404e+01	-3.63421e+04
3.36499e+01	-3.93401e+04	3.36499e+01	-3.97625e+04
3.45594e+01	-4.22104e+04	3.45594e+01	-4.26681e+04
3.54688e+01	-4.56203e+04	3.54688e+01	-4.61153e+04
3.63783e+01	-4.91860e+04	3.63783e+01	-4.97202e+04
3.72877e+01	-5.29466e+04	3.72877e+01	-5.35221e+04
3.81972e+01	-5.68965e+04	3.81972e+01	-5.75152e+04
3.91066e+01	-6.10354e+04	3.91066e+01	-6.16996e+04
4.00161e+01	-6.53528e+04	4.00161e+01	-6.60646e+04
4.09256e+01	-6.98785e+04	4.09256e+01	-7.06402e+04
4.18350e+01	-7.46257e+04	4.18350e+01	-7.54394e+04
4.27445e+01	-7.99135e+04	4.27445e+01	-8.07817e+04
4.36539e+01	-8.48777e+04	4.36539e+01	-8.58027e+04
4.45634e+01	-9.09396e+04	4.45634e+01	-9.19239e+04
4.54728e+01	-9.56890e+04	4.54728e+01	-9.67349e+04

C_p vs rotation

Export File Created with QBlade v0.96 64bit on 26.01.2022 at 21:03:03

Propeller clean Simulation		propeller icing Simulation	
Rot [rpm]	Ct	Rot [rpm]	Ct
1.81891e+01	3.51583e+02	1.81891e+01	3.48733e+02
1.90986e+01	3.86737e+02	1.90986e+01	3.83600e+02
2.00080e+01	4.22901e+02	2.00080e+01	4.19457e+02
2.09175e+01	4.61507e+02	2.09175e+01	4.57743e+02
2.18270e+01	5.05543e+02	2.18270e+01	5.01448e+02
2.27364e+01	5.42705e+02	2.27364e+01	5.38264e+02
2.36459e+01	5.85543e+02	2.36459e+01	5.80739e+02
2.45553e+01	6.30182e+02	2.45553e+01	6.25004e+02
2.54648e+01	6.76334e+02	2.54648e+01	6.70767e+02
2.63742e+01	7.24831e+02	2.63742e+01	7.18860e+02
2.72837e+01	7.73771e+02	2.72837e+01	7.67384e+02
2.81932e+01	8.24857e+02	2.81932e+01	8.18038e+02
2.91026e+01	8.78145e+02	2.91026e+01	8.70880e+02
3.00121e+01	9.32198e+02	3.00121e+01	9.24479e+02
3.09215e+01	9.88796e+02	3.09215e+01	9.80599e+02
3.18310e+01	1.04723e+03	3.18310e+01	1.03855e+03
3.27404e+01	1.10697e+03	3.27404e+01	1.09778e+03
3.36499e+01	1.18718e+03	3.36499e+01	1.17748e+03
3.45594e+01	1.23058e+03	3.45594e+01	1.22035e+03
3.54688e+01	1.29419e+03	3.54688e+01	1.28342e+03
3.63783e+01	1.36146e+03	3.63783e+01	1.35013e+03
3.72877e+01	1.42777e+03	3.72877e+01	1.41586e+03
3.81972e+01	1.49894e+03	3.81972e+01	1.48645e+03
3.91066e+01	1.56982e+03	3.91066e+01	1.55673e+03
4.00161e+01	1.64099e+03	4.00161e+01	1.62729e+03
4.09256e+01	1.71698e+03	4.09256e+01	1.70265e+03
4.18350e+01	1.79211e+03	4.18350e+01	1.77713e+03
4.27445e+01	1.88703e+03	4.27445e+01	1.87140e+03
4.36539e+01	1.95832e+03	4.36539e+01	1.94202e+03
4.45634e+01	2.06791e+03	4.45634e+01	2.05093e+03
4.54728e+01	2.11205e+03	4.54728e+01	2.09437e+03

C_m vs rotation

Export File Created with QBlade v0.96 64bit on 26.01.2022 at 21:06:50

Propeller clean Simulation		propeller icing Simulation	
Rot [rpm]	Cm	Rot [rpm]	Cm
1.81891e+01	-3.13971e+01	1.81891e+01	-3.17285e+01
1.90986e+01	-3.45557e+01	1.90986e+01	-3.49214e+01
2.00080e+01	-3.78477e+01	2.00080e+01	-3.82490e+01
2.09175e+01	-4.13013e+01	2.09175e+01	-4.17399e+01
2.18270e+01	-4.51007e+01	2.18270e+01	-4.55784e+01
2.27364e+01	-4.86582e+01	2.27364e+01	-4.91766e+01
2.36459e+01	-5.25641e+01	2.36459e+01	-5.31248e+01
2.45553e+01	-5.66158e+01	2.45553e+01	-5.72205e+01
2.54648e+01	-6.08138e+01	2.54648e+01	-6.14646e+01
2.63742e+01	-6.51740e+01	2.63742e+01	-6.58725e+01
2.72837e+01	-6.96677e+01	2.72837e+01	-7.04157e+01
2.81932e+01	-7.43167e+01	2.81932e+01	-7.51158e+01
2.91026e+01	-7.91335e+01	2.91026e+01	-7.99855e+01
3.00121e+01	-8.40742e+01	3.00121e+01	-8.49810e+01
3.09215e+01	-8.91931e+01	3.09215e+01	-9.01558e+01
3.18310e+01	-9.44639e+01	3.18310e+01	-9.54845e+01
3.27404e+01	-9.98700e+01	3.27404e+01	-1.00950e+02
3.36499e+01	-1.06325e+02	3.36499e+01	-1.07466e+02
3.45594e+01	-1.11080e+02	3.45594e+01	-1.12284e+02
3.54688e+01	-1.16975e+02	3.54688e+01	-1.18244e+02
3.63783e+01	-1.22965e+02	3.63783e+01	-1.24300e+02
3.72877e+01	-1.29138e+02	3.72877e+01	-1.30542e+02
3.81972e+01	-1.35468e+02	3.81972e+01	-1.36941e+02
3.91066e+01	-1.41943e+02	3.91066e+01	-1.43487e+02
4.00161e+01	-1.48529e+02	4.00161e+01	-1.50147e+02
4.09256e+01	-1.55286e+02	4.09256e+01	-1.56978e+02
4.18350e+01	-1.62230e+02	4.18350e+01	-1.63999e+02
4.27445e+01	-1.70029e+02	4.27445e+01	-1.71876e+02
4.36539e+01	-1.76828e+02	4.36539e+01	-1.78756e+02
4.45634e+01	-1.85591e+02	4.45634e+01	-1.87600e+02
4.54728e+01	-1.91378e+02	4.54728e+01	-1.93470e+02

C_n vs propeller radius (partial selection)

Export File Created with QBlade v0.96 64bit on 26.01.2022 at 21:05:15

pos [m]	Cn	pos [m]	Cn
5.14671e-02	3.41813e-02	5.14671e-02	3.08218e-02
5.14671e-02	3.08218e-02	5.14671e-02	2.87991e-02
5.58598e-02	4.76439e-02	5.58598e-02	4.35905e-02
5.58598e-02	4.35905e-02	5.58598e-02	4.00628e-02
6.31523e-02	4.58045e-02	6.31523e-02	4.20451e-02
6.31523e-02	4.20451e-02	6.31523e-02	3.87924e-02
7.33018e-02	4.03834e-02	7.33018e-02	3.72505e-02
7.33018e-02	3.72505e-02	7.33018e-02	3.45285e-02
8.62488e-02	3.48793e-02	8.62488e-02	3.22565e-02
8.62488e-02	3.22565e-02	8.62488e-02	2.99453e-02
1.01917e-01	2.98897e-02	1.01917e-01	2.76319e-02
1.01917e-01	2.76319e-02	1.01917e-01	2.56290e-02
1.20215e-01	3.18929e-02	1.20215e-01	3.00860e-02
1.20215e-01	3.00860e-02	1.20215e-01	2.86672e-02
1.41035e-01	1.27271e-01	1.41035e-01	1.25376e-01
1.41035e-01	1.25376e-01	1.41035e-01	1.23676e-01
1.64255e-01	3.26282e-01	1.64255e-01	3.24057e-01
1.64255e-01	3.24057e-01	1.64255e-01	3.22063e-01
1.89739e-01	4.87896e-01	1.89739e-01	6.21311e-01
1.89739e-01	6.21311e-01	1.89739e-01	5.10598e-01
2.17337e-01	4.20703e-01	2.17337e-01	4.18895e-01
2.17337e-01	4.18895e-01	2.17337e-01	4.17258e-01
2.46887e-01	4.06810e-01	2.46887e-01	4.05231e-01
2.46887e-01	4.05231e-01	2.46887e-01	4.03802e-01
2.78216e-01	3.91157e-01	2.78216e-01	3.89768e-01
2.78216e-01	3.89768e-01	2.78216e-01	3.88357e-01
3.11140e-01	3.75153e-01	3.11140e-01	3.73878e-01
3.11140e-01	3.73878e-01	3.11140e-01	3.72722e-01
3.45466e-01	3.57666e-01	3.45466e-01	3.56533e-01
3.45466e-01	3.56533e-01	3.45466e-01	3.55509e-01